



In silico ADMET, molecular docking and molecular simulation-based study of glabridin's natural and semisynthetic derivatives as potential tyrosinase inhibitors

Arti Kumari¹ · Rakesh kumar² · Gira Sulabh³ · Pratishtha Singh⁴ · Jainendra Kumar⁵ · Vijay Kumar Singh² · Krishna Kumar Ojha²

Received: 8 January 2022 / Accepted: 24 March 2022

© The Author(s), under exclusive licence to Institute of Korean Medicine, Kyung Hee University 2022

Abstract

Hyper-pigmentation conditions may develop due to erroneous melanogenesis cascade which leads to excess melanin production. Recently, inhibition of tyrosinase is the main focus of investigation as it majorly contributes to melanin production. This inhibition property can be exploited in medicine, agriculture, and in cosmetics. Present study aims to find a natural and safe alternative molecule as tyrosinase inhibitor. In this study, human tyrosinase enzyme was modelled due to unavailability of its crystal structure to look into the degree of efficacy of glabridin and its 15 derivatives as tyrosinase inhibitor. Docking was performed by *Autodock Vina* at the catalytic core enzyme. Glabridin effects on melanoma cell lines was also elucidated by analysing cytotoxicity and effect on melanin production. Computational ADME analysis was done by SwissADME. Molecular dynamic simulation was also performed to further evaluate the interaction profile of these molecules and kojic acid (positive inhibitor) with respect to apo protein. Notably, four derivatives 5'-formylglabridin, glabridin dimer, 5'-prenyl glabridin and R-glabridin exhibited better binding affinity than glabridin. Glabridin effectively inhibited melanin production in a dose dependent manner. Among these, 5'-formylglabridin displayed highest binding affinity with docking score -9.2 kcal/mol. Molecular properties and bioactivity analysis by Molinspiration web server and by SwissADME also presented these molecules as potential drug candidates. The study explores the understanding for the development of suitable tyrosinase inhibitor/s for the prevention of hyperpigmentation. However, a detailed in vivo study is required for glabridin derivatives to suggest these molecules as anti-melanogenic compound.

✉ Arti Kumari
arti.mbio@patnawomenscollege.in

Rakesh kumar
rakeshbis@cub.ac.in

Gira Sulabh
gira23yadav@gmail.com

Pratishtha Singh
rai.pratishtha86@gmail.com

Jainendra Kumar
jainendrak@gmail.com

Vijay Kumar Singh
vksingh@cub.in

Krishna Kumar Ojha
kris@cub.ac.in

¹ Department of Biotechnology, Patna Women's College, Patna, Bihar, India

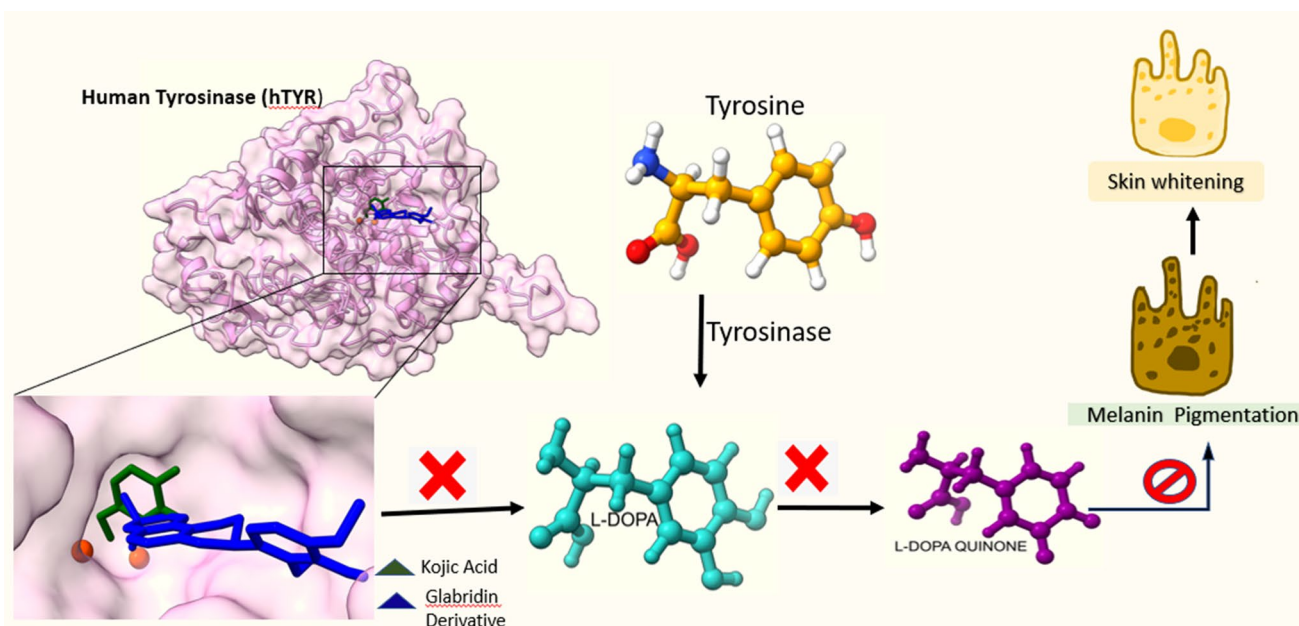
² Department of Bioinformatics, Central University of South Bihar, Gaya, Bihar, India

³ Department of Pharmacology, Manipal TATA Medical College, Manipal Academy of Higher Education, Jamshedpur, Manipal, India

⁴ School of Life Sciences, Jawaharlal Nehru University, New Delhi, India

⁵ Patliputra University, Patna, Bihar, India

Graphical abstract



Keywords Hyperpigmentation · Melanogenesis · Tyrosinase · Glabridin · 5'-formylglabridin · Kojic acid · Molecular simulation · Docking · Melanoma · Skin whitening

Introduction

Glabridin {systematic name: 4-[(3R)-8,8-dimethyl-3,4-dihydro-2H-pyrano[2,3-f]chromen-3-yl]benzene-1,3-diol} is a polyphenolic flavonoid compound from liquorice (*Glycyrrhiza glabra*, Fabaceae). It was first characterized in 1976 (Saitoh et al. 1976). Glabridin has been reported as main iso-flavanoid of licorice and its content in dried roots varies from 0.08 to 0.35% (w/w) (Simmler et al. 2013; Hayashi et al. 2003). Glabridin is known as species specific marker compound of *Glycyrrhiza glabra* Linn and is absent in certain species of the *Glycyrrhiza* genus (Lim, 2016). It also has phytoestrogen properties and displays broad range of biological activities. Several studies have reported pharmacological activities of glabridin mainly in terms of antibacterial (Kumari et al. 2020, 2019a; Fukai et al. 2002), antifungal (Gupta et al. 2008), anti-oxidant (Fukai et al. 2000), anti-inflammatory, antiviral, anti-allergenic, neuroprotective (Cui et al. 2008), anti-osteoporotic (Yu et al. 2008), anti-tumorigenic properties (Choi, 2005; Hsu et al. 2011). Damle (2014) and Simmler (2013) reviewed pharmacological properties of *Glycyrrhiza glabra* and also talked about skin whitening properties of *G. glabra* extracts. The role of glabridin in skin whitening needs more investigation. There has been a research gap after the study performed by Yokata et al. 1998 which state that glabridin contains two hydroxyl

groups which are important for the inhibition of tyrosinase and melanin synthesis. The hydroxyl group at the 4' position is more closely related to the inhibition (Yokota et al. 1998). Melanin absorbs harmful ultraviolet radiations (UVR) and protects the skin (Pillaiyar et al. 2018). Conglomeration of melanin pigments leads to hyper-pigmentary disorders (Cestari et al. 2014). Melasma, post inflammatory hyper pigmentation, *Café- au- lait*, age spots, solar lentigo, erythema dyschromicum perstans, *prurigo pigmentosa*, *Linea niagra*, freckles, lentigenes are common dermatological problems (Baurin et al. 2002) and don't have the advance treatment strategies presently.

Tyrosinase (EC.1.14.18.1, Syn. Polyphenol oxidase) is the key enzyme of the Melanogenesis pathway and catalyses the conversion of tyrosine into dihydroxyphenylalanine (DOPA), and then, DOPA into dopaquinone (Shi et al. 2002; Kobayashi et al. 1995). Both steps are rate limiting reactions of the melanin biosynthesis pathway (Kumari et al. 2019b; Radhakrishnan et al. 2013; Raper, 1928; Kobayashi et al. 1995; Borges et al. 2001). As over-expression of brain tyrosinase catalyses production of dopaquinones in the process of age-dependent neuromelanin production, which in excess leads to neuronal damage, implicating the tyrosinase potential in neurodegenerative diseases like Parkinson's and Huntington's diseases (Pillaiyar et al. 2017; Cavalieri et al. 2002; Vontzalidou et al.

2012; Hasegawa et al. 2010; Tessari et al. 2008; Greggio et al. 2005; Nithitanakool et al. 2009). Tyrosinase has also been associated with the browning of vegetables and fruits during post-harvest and handling processes, leading to quick degradation (Yi et al. 2010; Friedman, 1996; Mayer, 1986). The role of tyrosinase has been further explored in the moulting process of insects and wound healing (Liu et al. 2007; Pillaiyar et al. 2017). Structurally, this multifunctional enzyme's catalytic core has two copper (III) atoms, surrounded by three histidine residues which act as catalytic centre of the enzyme (Matoba et al. 2006; Masum et al. 2019). The most prominent approach for the development of melanogenesis inhibitors is the down regulation of tyrosinase as strong correlation has been observed between tyrosinase and melanin pigmentation (Masum et al. 2019; Pillaiyar et al. 2017). Targeting tyrosinase is the key to comprehend the knowledge of melanin inhibition mechanism which can help to improve hyper pigmentary conditions (Lee et al. 2020). Several tyrosinase inhibitors are reported as potential therapeutic and cosmetic agents for various hyperpigmentation conditions and skin related issues respectively. Tyrosinase inhibitors can stumple the high tyrosinase activity and play notable role as remedies for skin disorders (Pillaiyar et al. 2017). Apart from their role in medicine, tyrosinase inhibitors have attracted much attention in the cosmetic industry (Pillaiyar et al. 2017).

Nature has always been a great reservoir of the novel compounds which can be exploited to obtain various drugs (Mushtaq et al. 2018) and these phytochemicals and their derivatives are naturally produced by plants as secondary metabolites which helps in defence against pathogens (Isah 2019, Kumari et al. 2021). Several studies have reported better results from derivatives in the treatment of diseases than the parent compound (Haudecoeur et al. 2017). However, in medicine, tyrosinase inhibitors are important clinical antimelanoma drugs but only a few compounds are effective and safe. Thus, the hunt for safe cosmetic agents demands identification of new molecules/substance with more powerful actions, and without any side effect (Ali and Naaz 2015). Thus, to enhance the knowledge of anti-melanogenic natural compounds, we have conducted the virtual docking studies of glabridin and its various structural derivatives with the modelled human tyrosinase enzyme (hTYR) to evaluate their anti-tyrosinase efficacy and thus they could potentially prevent abnormal pigmentation. It also reports the effect of glabridin on the melanoma cells for its anti-melanogenic potentiality. The aim of the current study is to find a suitable candidate for the development of new skin whitening agent for hyper pigmentary disorders or cosmetic purpose which may have lesser adverse effects.

Materials and methods

The effort was to find the anti-tyrosinase molecule using derivatives of glabridin. This study includes the natural compounds present in *Glycyrrhiza glabra* plant which are proposed to have anti-tyrosinase activity in traditional usages. All derivatives included in the study are (R)- glabridin [4484219], 5'-prenyl glabridin [23641093], 2',4'-O- dimethyl glabridin [480856], glabridin dimer [5481978], R- Hispaglabridin A [4484221], R-Hispaglabridin B [5318057], 5'-formylglabridin [46230506], 4'-O-Methyl preglabridin [44257508], 4'-O-prenyl glabridin [480861], 4'-O-methyl glabridin [5319664], 3'-hydroxy-4'methoxy glabridin [10338211], 2'-O-methylglabridin [74830193], 2'-O,5'-C-diprenylglabridin [480868], Hispaglabridin A [442774] and Hispaglabridin B [15228661]. These are structural derivatives of glabridin and can be obtained from the extract of *Glycyrrhiza glabra* plant by HPLC purification except Glabridin dimethyl ether (2',4'-O- dimethyl glabridin) and 2'-O-methylglabridin. These two compounds are semisynthetic and Belinky et al. (1998) synthesized them by the following method. Glabridin (100 mg, 0.31 mmol) in a round bottom flask was dissolved in acetone (2 ml) and methyl iodide (30 ml, 0.33 mmol) and K₂CO₃ (64 mg, 0.46 mmol) were added. The reaction mixture was heated to 50 °C with stirring, and after 6 h, the conversion reaction was determined by HPLC analysis. Glabridin (35%), 2'-O-methylglabridin (30%), 4'-O-methylglabridin (20%) and 2',4'-O-dimethylglabridin (15%) were obtained. These compounds were separated and purified on a silica gel column, using CH₂Cl₂ and then CH₂Cl₂/3% CH₃OH as eluents. 2',4'-O-dimethylglabridin can be synthesized in a higher yield by using excess of methyl iodide and potassium carbonate in the initial reactions. Kojic acid was used as positive control for the docking studies and for in vitro studies glabridin (62% pure) was purchased from Kan Phytochemicals Pvt. Ltd.; Sonipat, Haryana. The experimental workflow employed is displayed in Fig. 1.

Homology modelling of hTYR and secondary structure prediction

Due to non-availability of an experimentally established high-resolution X-ray crystal structure of hTYR in the Protein Data Bank, a three-dimensional structural model of the same was built using MODELLER (Webb et al. 2014) based on homology modelling. Tyrosinase protein sequence (Homo sapiens) (Accession no AAB60319.1) was retrieved from the NCBI protein database (<https://www.ncbi.nlm.nih.gov>) (Johnson et al. 2008) and used as

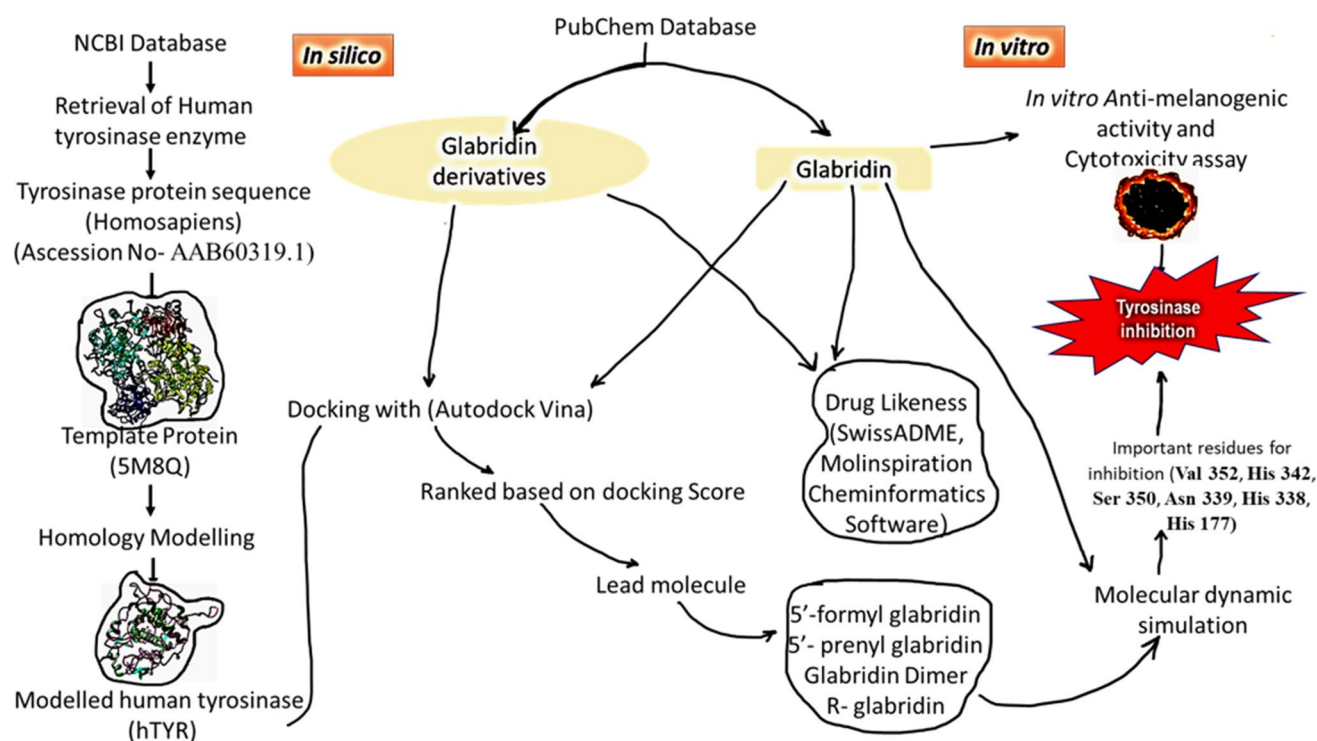


Fig. 1 Experimental workflow employed during the present study

query sequence to perform BLASTp. A structural model of the human tyrosinase was constructed using MODELLER using published crystal structure of 5, 6-dihydroxyindole-2-carboxylic acid oxidase of human RCSB Protein Data Bank (Berman et al. 2007) (PDB ID: 5M8Q). The modelling template showed maximum 44.44% identity and query coverage 81%. Modelling was done for the catalytic domain by removing 25 amino acids from the start along with a short sequence of 59 residues from 471 to 529 of the peptides. Two copper molecules were added to the catalytic centre obtained from Bacterial tyrosinase (Matoba et al. 2006). The overall quality of the modelled structure was validated through the Ramachandran plot using Rampage server. The secondary structure of the human tyrosinase enzyme sequence was also determined by self-optimized prediction method (SOPMA) (Combet et al. 2000). The secondary structure of protein is important to understand the three-dimensional structure of the protein and its function. The default parameters of window width 17, similarity threshold 8 and number of states 4 were used for this study.

Structure preparation of ligands and target modelled hTYR

Glabridin and its derivatives (supplementary data-Table 1S) were retrieved from PubChem database to investigate their

possible impact as inhibitor of human tyrosinase. 3D structures of glabridin derivatives were downloaded in sdf format. The sdf files were converted into pdbqt file format using open babel tool on Linux version 16.04.

Active site prediction and molecular docking of ligands with modelled hTYR

Active site prediction was performed by CastP web server (Tian et al. 2018). Docking studies were carried out on *Autodock Vina* (Trott and Olson 2010) which carries out automated preparation steps for both receptor and ligands that include the addition of partial charges and required hydrogen atoms. Docking of ligand molecules was performed on predefined grid obtained from the template structure in complex with kojic acid (Lai et al. 2017). The grid size was $50 \times 50 \times 50$ and dimension for X, Y and Z coordinates – 15.715, 5.183 and – 20.640, respectively. These parameters were also used to dock glabridin derivatives using *Autodock Vina* executed on Linux platform. The docking was validated by best possible conformation of each ligand and the best confirmation of each compound was selected based on the lowest docking score and their binding interactions measured in terms of Gibbs free energy (ΔG). The docked structures (protein–ligand complexes) stabilize through several binding interactions such as polar, hydrophobic, hydrophilic, pi-pi stacking, salt bridge etc. The

molecular interactions were analysed and evaluated based on their polar and hydrophobic interactions using structure visualization tool *Pymol* version 2.3 (DeLano 2002), Chimera10.1 (Pettersen 2004) and *LigPlot* (Wallace et al. 1995).

Anti-melanogenic activity of glabridin on melanoma cell line

The anti-melanogenic activity of glabridin was evaluated on B16F10 cell line. The cytotoxicity of glabridin on murine melanoma cell lines (B16 melanoma cells) and effect of glabridin concentrations on the melanin production by melanoma cells was observed.

Effect of glabridin on Melanin production by B16 melanoma cells

Melanin contents in cultured B16 melanoma cells were measured according to the method of Oikawa et al. (1973) with slight modifications. B16 melanoma cells were seeded (initial density of cells 0.4×10^4 cells/cm²) in T75 culture flasks, and glabridin was added to the culture medium with concentrations from 1.0 to 5 µg/ml. After 3 days culture, the cells were collected by brief trypsinization and subsequent centrifugation, and then treated with 5% trichloroacetic acid, ethyl alcohol: diethyl ether (3:1) and diethyl ether successively in this order. The cells were dissolved with 2 M NaOH containing 10% DMSO. Doxorubicin was used as positive control. The melanin contents were measured with Agilent Cary 50 UV Visible spectrophotometer at 400 nm. Results were analysed statistically using statistical software *Prism 5* via one-way analysis of variance at $P < 0.05$ with control.

Cell viability assay (MTT assay)

B16F10 cells were grown to confluence in T75 cm² flask supplemented with Dulbecco's Modified Eagle Medium and 10% fetal calf serum in CO₂ incubator with 5% CO₂. Cells were seeded at a density of 1×10^4 cells per well in DMEM medium. Twenty-four hours post seeding, cells were treated at concentrations ranging from 5 to 200 µg/ml of glabridin for different time intervals (24 and 48 h). After the exposure times, MTT was added to a final concentration of 0.5 mg/ml medium and the plates were incubated for 4 h at 37 °C. The purple formazan crystals formed were dissolved in DMSO and read at 570 nm in a micro-quant plate reader. The assay was carried out in triplicates. The results were expressed as % inhibition.

Drug likeness and In-silico ADME prediction

Early detection of ADME properties reduces the failure in clinical phases and also minimises the load of synthesis of compounds for testing its potentiality for drug. Hence, it has become a vital tool in drug candidate identification. On this note, in silico prediction of the ADME properties (absorption, distribution, metabolism and excretion) was performed using SwissADME web tool (Daina et al. 2017) to determine the activity of these molecules within human body. These pharmacokinetic parameters were evaluated for the glabridin and its 15 derivatives to investigate their drug candidate chance. SMILES of each compound was obtained from PubChem database and was used for the analysis. The drug likeness of the molecules was predicted by adopting Lipinski's Rule of 5. The rule of 5 predicts molecules with more than 5H-bond donors, 10-H bond acceptors, molecular weight more than 500 Da and the logP greater than 5 likely to had poor absorption and permeation of molecular entities (Ibrahim et al. 2020).

Molecular dynamics simulation study

MD simulation has been performed using GROMACS 5.1.2. (Berendsen et al. 1995) to analyse the structural stability of tyrosinase upon ligand binding, under GROMOS96 43a1 force field (Pol-Fachin et al. 2009). MD simulations for apo-protein (TYR) along with all of the receptor-ligand complexes, TYR-Kojic acid, TYR-5'- formylglabridin, TYR-5' prenylglabridin, TYR- Glabridin dimer, TYR- 3'-hydroxy-4'-methoxyglabridin and TYR- (R)-glabridin, were performed in triclinic periodic boundary conditions. The topologies for ligand molecules were prepared using PRODRG (Schüttelkopf and Van Aalten 2004). The systems were prepared with solvation using SPC water model at 1 nm marginal radius, followed by neutralization by adding the significant number of Na⁺ ions. The final systems, consisted of Protein, Ligand (except for TYR), Na⁺ ions and solvent, was subjected to energy minimization step for each system was performed using steepest decent integrator for 5000 iterations using the 0.01 energy step. After that, NVT (Berendsen et al. 1995) and NPT (Berendsen et al. 1984) ensembles were employed for temperature and pressure coupling and equilibration with leap-frag integrator for 50,000 steps (100 ps). Finally, 50,000 ps production simulations of each system were performed 2 fs time interval (Millan et al. 2017). The RMSD of backbone, RMSF of C-alpha atoms, SASA, R_g, and hydrogen bond were retrieved from MD simulation trajectories, and analysis plots were prepared using OriginPro.

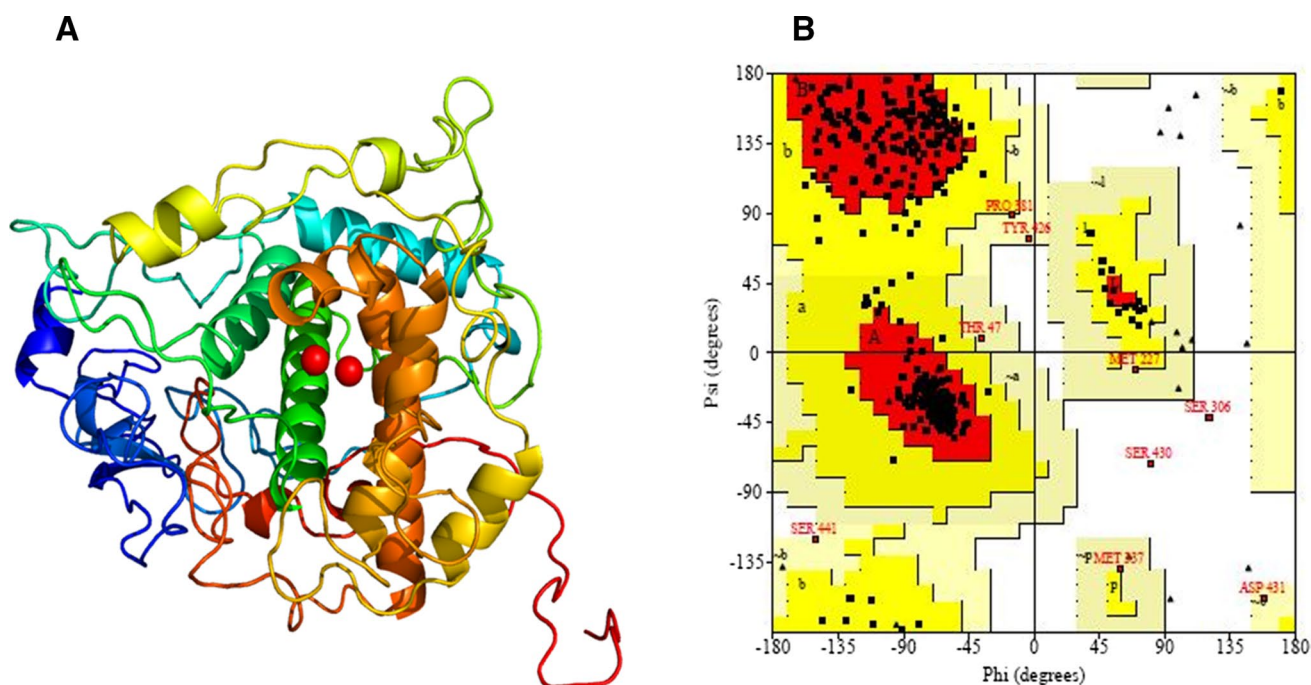


Fig. 2 **A** Three-dimensional structure of the modelled human tyrosinase (hTYR) (Two red dots in the centre represents Copper metal ions essential for the catalytic activity), **B** The Ramachandran plot for the modelled protein: the residues occurring red coloured region are

in allowed region, residues in yellow region are in generously allowed region. (97% residues are in the allowed region where as 1.6% residues are in generously allowed region)

Result and discussions

Homology modelling

Homology modelling of hTYR was successfully done. Stereo chemical properties of 3D protein structure of hTYR, obtained through the structure model algorithm (Fig. 2A) and validated with several validation tools associated with save server, were analysed through the Ramachandran plot. Ramachandran plot analysis indicated that more than 90% amino acid residues accommodate in the allowed region (Fig. 2B). These properties improved after energy minimization through YASARA server and 94% residues lay in the allowed region of Ramachandran plot. As the tyrosinase activity is dependent on the presence of two copper ions, they were added to the catalytic centre from the bacterial tyrosinase (Lai 2017). Secondary structure prediction results (Sup Table 2S) and homology model were analogous to each other. Majority of studies have implicated mushroom tyrosinase and bacterial tyrosinase (da Silva et al. 2017; Lima et al., 2014; Radhakrishnan et al. 2013). However, differences in the binding pockets of mushroom and human tyrosinase have been reported (Garcia -Borron, 2002). Only few researchers have reported modelling of human tyrosinase enzyme (Lee et al., 2020; Nokinsee et al. 2015) but in their modelling studies, the template similarity was very low.

Nokinsee et al. (2015) used protein template, tyrosinase of *B. megaterium* (PDB Id- 3NQ1) which had highest identity with human tyrosinase of only 33.5%, whereas in present study template used for homology modelling is Human tyrosinase related protein (PDB ID 5M8Q) which showed 44.6% identity with hTYR.

Interaction study between protein and ligand complexes

Active site prediction by Cast p resulted in several active sites. Among major active sites, site 1 active site was found to be the largest pocket. Kojic acid binding coordinates with template protein were similar to the coordinates of site1 active site of modelled enzyme. The docking of the glabridin and its derivatives was successfully achieved with the *Autodock vina* tools and the results were analysed in term of the binding energy. The docking results of Glabridin and kojic acid are presented in Fig. 3 (3A—glabridin and hTYR docking; 3B—Kojic acid and hTYR docking). Docking scores in terms of binding affinity for glabridin and its derivatives are presented in Table 1. Docking structures of the molecules which showed lesser docking energy score than glabridin are presented in Fig. 4A, B, C and D. Cast P analysis of docked structures of these molecules also confirmed that all ligand

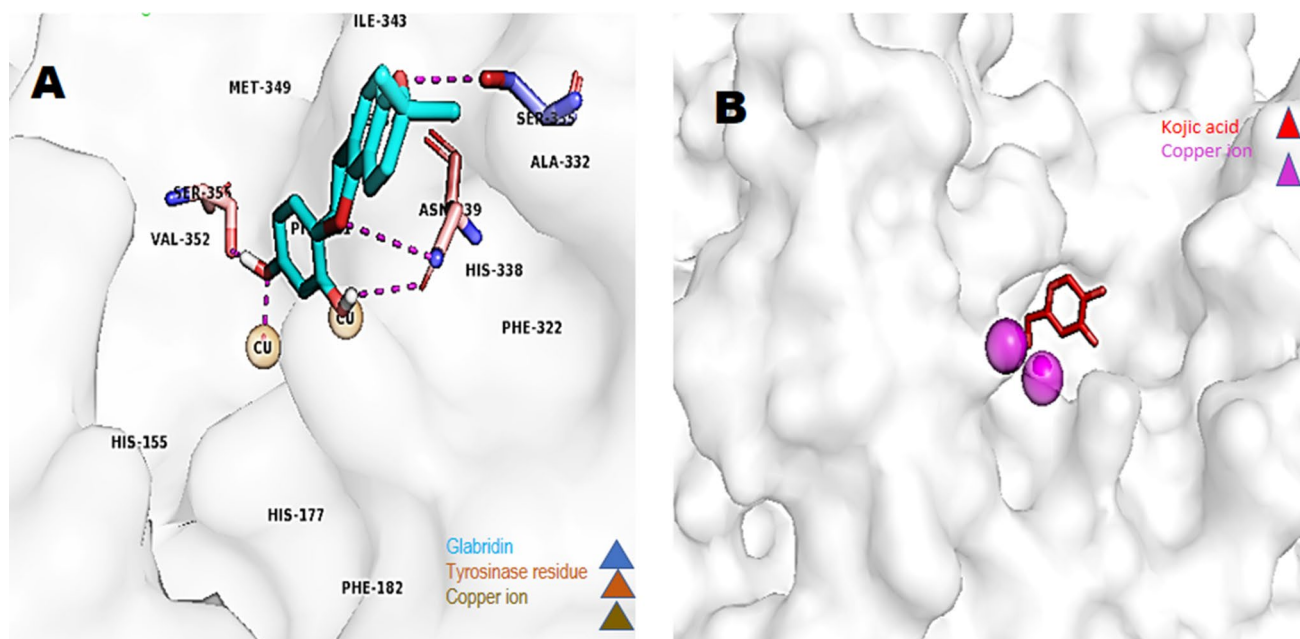


Fig. 3 Docking structure of ligands (Glabridin and Kojic acid). **A:** Docking picture of glabridin with modelled hTYR, **B:** Docking picture of Kojic acid with modelled hTYR

Table 1 List of glabridin & glabridin's derivatives and Kojic acid with their docking score (Gibb's free energy)

Name of Ligand	Dock Score (Gibb's free energy)
3'- hydroxy 4' methoxy-glabridin	-8.0
4'-O- methylglabridin	-7.6
4'-O-prenyl glabridin	-8.0
4'-methyl preglabridin	-7.6
5'- formylglabridin	-9.3
5'- prenylglabridin	-8.8
2'-O, 5'-C-diprenyl glabridin	-8.6
Glabridin dimethylether	-7.6
Glabridin dimer	-9.2
Hispaglabridin A	-7.9
2'-O- methylglabridin	-8.1
(R)-glabridin	-8.9
(R)- hispaglabridin A	-8.0
(R)- hispaglabridin B	-8.6
Hispaglabridin B	-7.9
Glabridin	-8.8
Kojic Acid	-6.8

molecules were docked in the active pocket (site 1) of the modelled tyrosinase and amino acid composition of this site is presented in Table 3S (suppl). Few representative glabridin derivative molecules bound in the active pocket 1 has been presented in Fig. 5. Glabridin and its

all 15 derivatives were docked in the active pocket of the enzyme which indicate that they may interfere with tyrosinase activity. The hydrophobic interaction of these ligand molecules along with kojic acid was calculated using *Lig-Plot* and generated interactions are shown in Fig. 6 (where the ray like structures represent the hydrophobic relationship between the atoms as well as the molecules) except for glabridin dimer due its complex structure. The hydrophobic interaction was calculated within the 4 Å region around ligand molecules.

Among all derivatives, 5'-formylglabridin comes out to be the best molecule based on its docking score (-9.3). Other important molecules which can be analysed in vivo for their anti-tyrosinase activity along with 5'-formylglabridin are glabridin dimer, 5'-prenyl glabridin and (R)-glabridin which showed attractive binding modes with docking scores -9.2, -8.8, -8.9 and -8.6 respectively. Glabridin binds to tyrosinase by forming totally 3 hydrogen bonds with residue SER355, ASN 339, Cu 501, where C'2 of glabridin binds to SER355 and Cu501, C'4 of glabridin binds to ASN339. This is in agreement with study of Yokata et al. 1998. It can be inferred that both group of glabridin are important for the inhibition activity of the glabridin. Cu forms the active centre of the enzyme. Hence, glabridin interfere with the tyrosinase activity. This study revealed the anti-tyrosinase property of glabridin and its derivatives. Our study shows that, the amino acids involved in the H-bonding with kojic acid are not involved in the H-bonding with glabridin whereas those residues are involved in other type

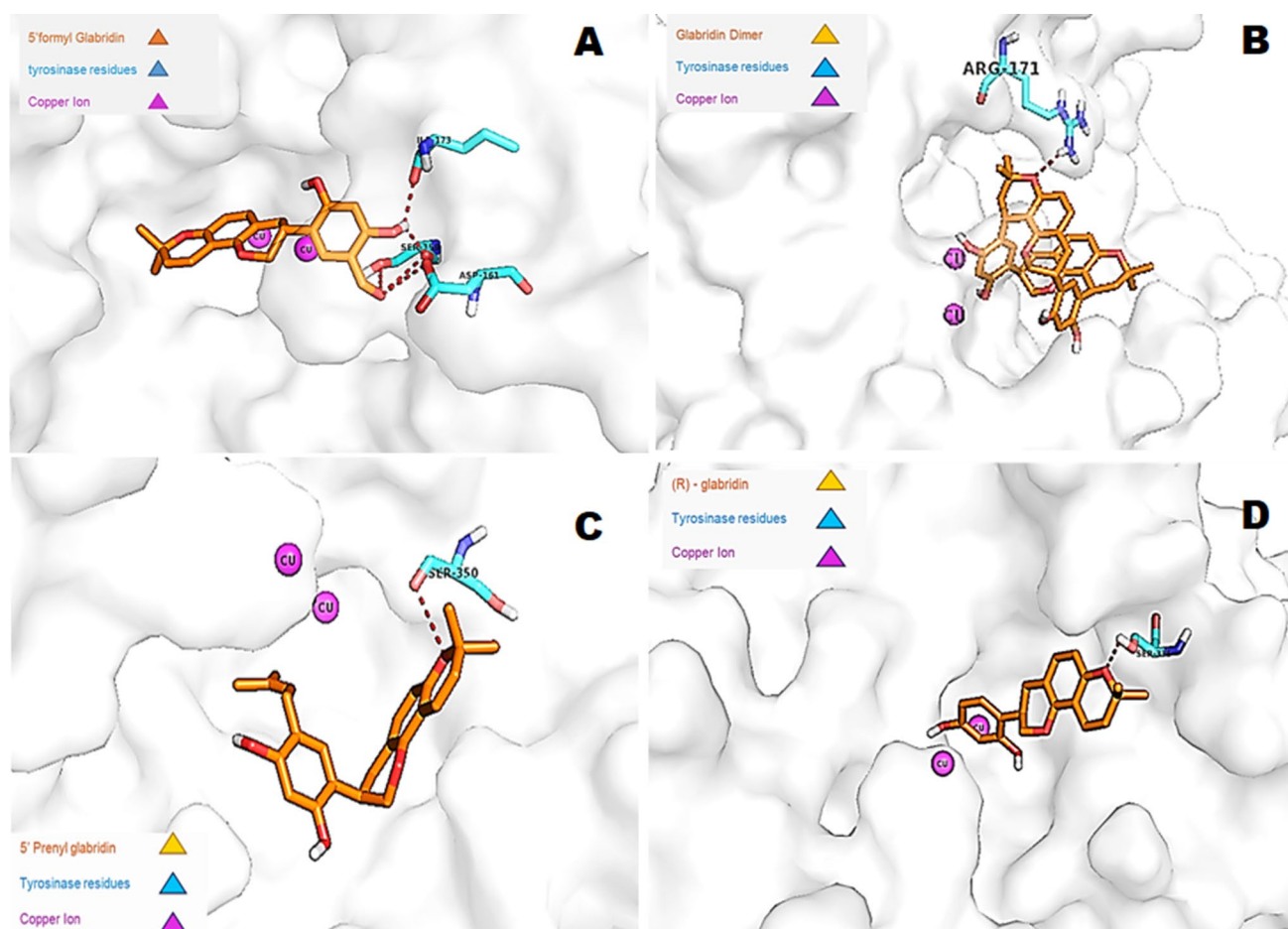


Fig. 4 Docking structure of glabridin derivatives- **A:** 5'-formylglabridin ligand docked with modelled hTYR (Dock score: -9.3), **B:** Glabridin dimer ligand docked with modelled hTYR (Dock

Score: -9.2), **C:** 5' prenylglabridin ligand docked with modelled hTYR (Dock Score: -8.8), **D:** (R)—Glabridin ligand docked with modelled hTYR (Dock score: -8.9)

of interactions and this may suggest the non-competitive inhibition mechanism. This result is in accordance with the reports of Chen et al. 2016. We comparatively analysed the stability of glabridin, kojic acid, 5'-formyl glabridin, R- glabridin, 5' -prenylglabridin and 3-Hydroxy- 4' methoxy binding with human tyrosinase and report the interacting residues in Table 2. Interacting residues of other molecules are tabulated in Suppl. Table 4S. 5'- formylglabridin forms four hydrogen bonds with residues ARG 171, ASP 161, ILE 173, GLU 178, R- glabridin forms 3 H-bond with SER 355, ASN 339 and Cu 501 whereas 5' prenylglabridin forms only one hydrogen bond with ARG171. The binding mode of selected ligands in the active site of human tyrosinase model involved some very positive hydrophobic interactions. Important residues which are either involved in H-bonding or interact with other kind of interaction which are common with kojic acid are HIS 338, HIS 177, HIS 342, SER 350, VAL 352 and ASN 339 and possess very important role in interaction with these ligands. The residues which are limited to glabridin and its derivatives interaction are PHE

322, SER 330, SER 355, ILE 343, HIS 155, ARG 171 which could have important roles in the inhibition.

In vitro testing the effect of glabridin on to tyrosinase

Treatment of B16 melanoma cells with glabridin at concentration 1, 1.5 and 2 $\mu\text{g/ml}$ was found to decrease the melanin concentration effectively. Each group was statistically correlated with control as well as with other groups. Statistical analysis showed that the reduction in melanin content was highly significant at each treatment with respect to untreated cells. Analysis of significance level among different treatment showed that 2.5 $\mu\text{g/ml}$ was significant than 1.5 $\mu\text{g/ml}$ and similarly 2 $\mu\text{g/ml}$ was significant than 1 $\mu\text{g/ml}$ dosages of glabridin (Fig. 7A).

Cytotoxicity assay

Morphological changes were observed in melanoma cells exposed to glabridin and showed toxicity in concentration

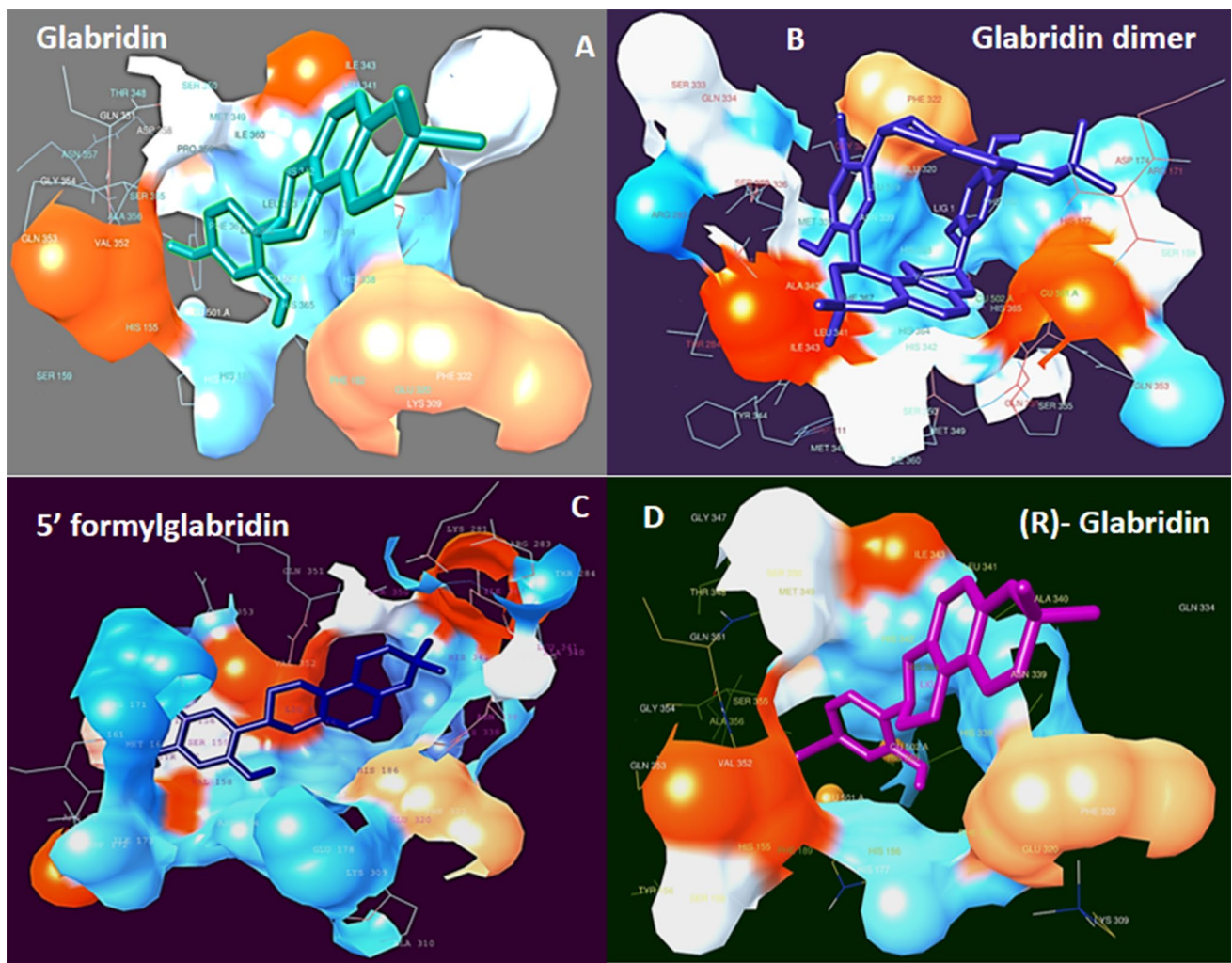


Fig. 5 Cast p generated files analysed in Chimera 10.1 which shows that all ligands were docked in the site 1 active pocket whereas the orientation of ligands are different

dependent manner (Fig. 7B). Glabridin was shown to inhibit the melanin production in dose dependent manner and 1 µg/ml of glabridin significantly inhibited the melanin production in comparison to the untreated cells as control. The cytotoxicity analysis of glabridin was analysed from 5 to 200 µg/ml. Dose dependent cytotoxicity showed by glabridin was calculated as percentage of inhibition (Supplementary data 1S and 2S). The effect of compounds on the capability of cells to replicate is used as an index of toxicity; IC₅₀ calculated for 24 h was 22.78 µg/ml, and for 48 h, it was

13.82 µg/ml which suggest that it could be efficiently used for the purpose (Supplementary data 3S).

Drug-likeness and in silico ADME prediction analysis

A molecule should fulfil certain criteria to become a potent drug molecule. Drug development procedure involves the assessment of ADME properties of a molecule which stands for absorption, distribution, metabolism and excretion. A potent molecule should reach the target in optimum

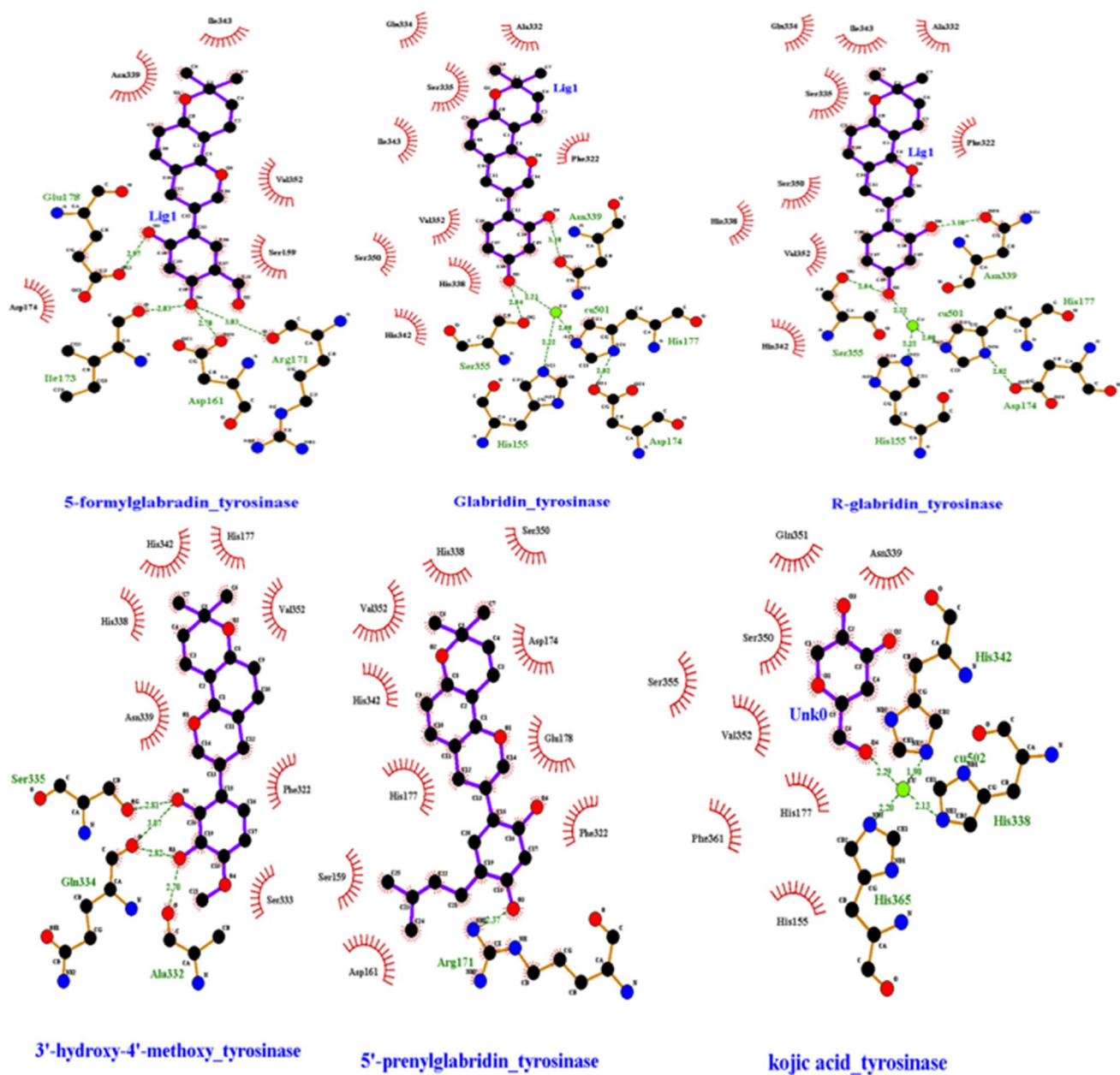


Fig. 6 Hydrophilic and hydrophobic interaction between ligand (glabridin, 5'- formylglabridin, Kojic acid, R- glabridin, 5'prenylglabridin and 3'-hydroxy -4' methoxyglabridin) with modelled hTYR

Table 2 Comparative analysis of molecular interaction of kojic acid and ligand molecules (Glabridin and its few derivatives) with tyrosinase enzyme

Interacting residues of modelled Tyrosinase enzyme in docked structure					
Ligand molecule	Hydrogen bonding residues	Bond length	Hydrophobic bond residues	Common interacting residues of glabridin and other dervatives (Similar to kojic acid)	Other interacting residues
Kojic acid	His 338	2.13	His 155, His 177, Ser 355, Ser 350, Met 349, Val 352, Gln 351, Asn 339	Val 352 His 342 Ser 350 Asn 339 His 338 His 177	Phe 322 Ser 330 Ser 355 Ile 343 His 155 Arg171
	His 365	2.20			
	His 342	1.90			
Glabridin	Cu	2.27	Phe 322, His 338, Val 352, His 342, Ser 350, Ile 343, Gln 334, Ser 335, Ser 333, Ala 332		
	His 155	2.22			
	Ser 355	2.90			
	His 177	2.08			
	Asn 339	3.04			
5'formyl glabridin	Arg 171	3.83	Ser 159, Leu254, Met 160, Val 352, Asp 174, Phe 322, His 177, His 342, Ile 343, Ser 350, Ser 335, Asn 339		
	Asp 161	2.70			
	Ile 173	2.83			
	Glu 178	2.97			
5'Prenyl glabridin	Arg171	2.37	Phe322, Glu178, Asp174, Ser350, His 338, Val 352, His 342, His 177, ser 159		
R- Glabridin	His155	2.22	Phe322, Ala322, Ile343, Glu334, Ser335, Ser350, Val 352, His342, His 338		
	Asp174	2.82			
	Asn339	3.10			
	His177	2.08			
3'-Hdroxy-4'- Methoxyglabridin	SER-335	2.81	Asn339, Ser333, Phe322, Val352, His177, His342, His338		
	SER-333	3.07,2.82			
	ALA-332	2.70			

concentration and stay there in bioactive form long enough for the expected biologic event to occur (Daina et al. 2017). Pharmacokinetics profile of the small molecule is important in drug discovery process. Swiss ADME results were categorised in 6 areas namely physiochemical properties, lipophilicity, water solubility, pharmacokinetics, drug likeness and medicinal chemistry. Bioavailability radar provides the first glance at the drug-likeness of a molecule. ADME results detailed in Table 3 reveals that, all derivatives of glabridin acquire acceptable drug like properties in addition to the other drug likeness parameters. All

derivatives satisfied all the rule, ($MW \leq 500$ Da, $\text{LogP} < 5$, $n\text{HBD} \leq 5$, $\text{NHBA} \leq 10$ and $\text{TPSA} < 140 \text{ \AA}^2$) except glabridin dimer which has molecular weight more than 500 Da and 2'-O,5'-C-diprenylglabridin whose log P value was higher than 4.15. All the compounds water solubility is moderate to poor. None of the compound are violating more than one rules of Rule 5 which is acceptable in case of natural compounds especially the molecular weight. All molecules have $\text{TPSA} < 140$, and most importantly the logKp which denotes the skin permeability is within the standard range of -8.0 to -1.0 . A parameter analysed by

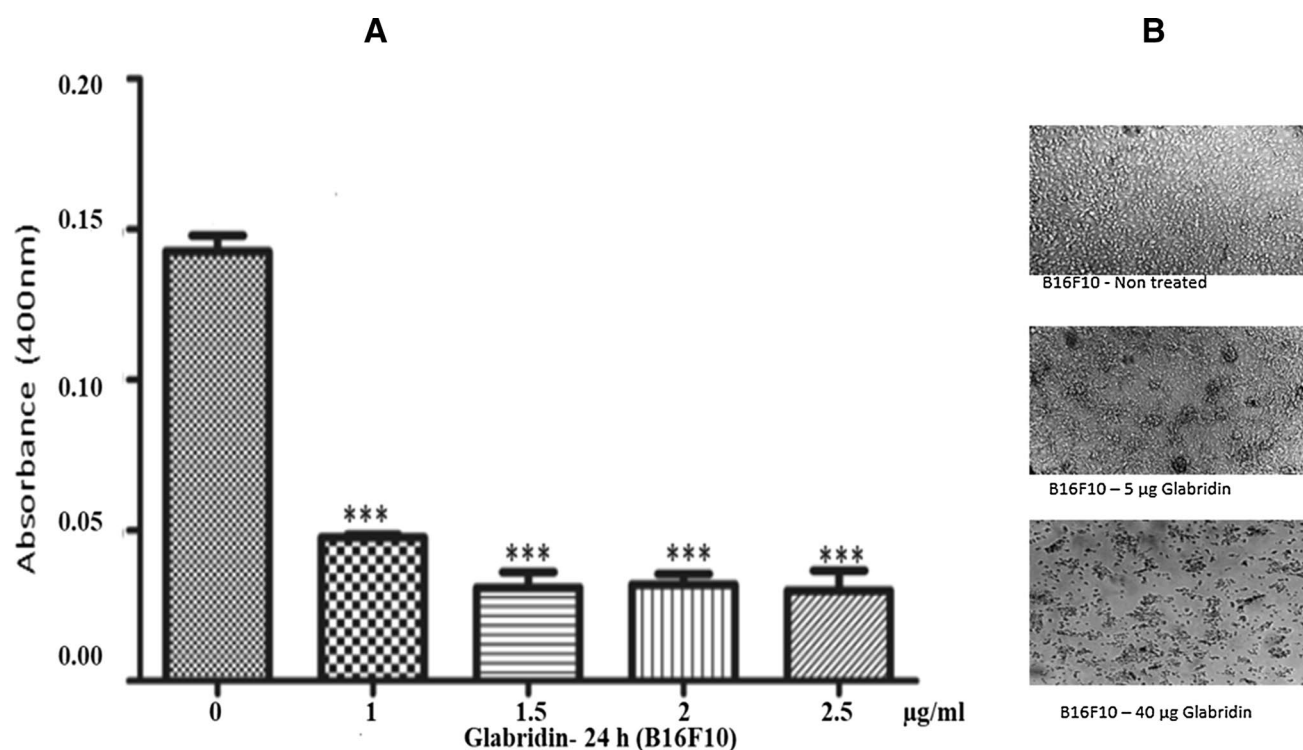


Fig. 7 Testing the effect of glabridin on melanin production in B16F10 melanoma cell lines; **A:** Effect of glabridin's different concentrations on melanin production is dose dependent. Significant reduction in melanin production was observed with increase in dosages, **B:** Effect of glabridin on cell viability. B16F10 cells were treated with varying concentrations of glabridin (5–200 µg/ml) for

24 h and 48 h. Bright field images were captured, and representative images for control and treatments are provided to indicate the morphological changes at two concentrations (5 and 40 µg) of glabridin. Cellular viability was measured via MTT assay and cell viability was calculated in percentage and IC 50 was also determined

Molinspiration web server is enzyme inhibition availability. All molecules have enzyme inhibition capability which ranged between 0.37 and 0.63. All the molecules included in this study showed the ADME parameters (Molecular weight, Log P, no of hydrogen bond donor, no of hydrogen bond acceptor, no of rotatable bond, TPSA, no Lipinski rule violation, Log Kp, Enzyme inhibition capability, Synthetic accessibility) results within favourable range. Thus, all have good oral bioavailability or permeability. Similar analysis was performed by Ibrahim et al. 2020 for some derivative molecules as elevators of p53 protein levels. Molecular properties and bioactivity analysis by Molinspiration web server (data tabulated as supplementary

material 5S) projected all molecules as enzyme inhibitor. All molecules in this study are projected as potential drug molecule. Even though majority of our molecules could be considered further for analysis as drug candidate based on ADME properties and calculation of molecular properties and bioactivity score prediction by Molinspiration web server, we present only few molecules [Glabridin, 5'-formylglabridin, 5'-prenylglabridin, Glabridin Dimer, R- Glabridin and 3'-hydroxy-4'-methoxyglabridin] having lower binding affinity score than glabridin for the molecular dynamic simulation studies in comparison to positive control kojic acid along with Apo protein.

Table 3 Lipinski properties of glabridin and its derivatives with SwissADME

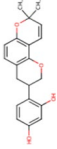

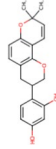

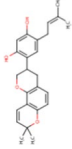

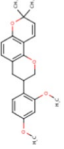

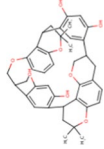

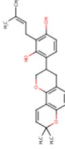

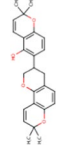

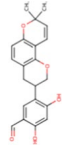

Name	MW	LogP	nHBD	nHBA	nRotB	TPSA	Lip Vio	Log Kp	EI	SA	2-D structure	Bio-rad
Glabridin	324.37	3.89	2	4	1	58.92	0	-5.52	0.50	4.04		
(R)- glabridin	324.37	3.89	2	4	1	58.92	0	-5.52	0.50	4.04		
5'prenyl glabridin	392.49	5.82	2	4	3	58.92	0	-4.56	0.54	4.58		
Glabridin dimethyl ether (2',4'-O-dimethyl glabridin)	352.42	4.54	0	4	3	36.92	0	-5.23	0.37	4.26		
Glabridin dimer	648.74	6.95	4	8	0	117.84	1	-5.23	0.58	6.44		
R- Hispa glabridin A	392.49	5.82	2	4	3	58.92	0	-4.56	0.63	4.58		
R-Hispa glabridin B	390.47	5.17	1	4	1	47.92	0	-5.01	0.42	4.45		
5'-formyl glabridin	352.38	3.90	2	5	2	75.99	0	-5.68	0.39	4.06		

Table 3 (continued)

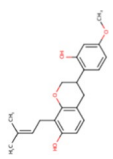

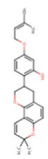

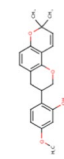
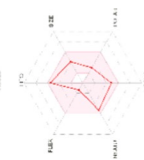
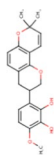

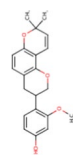

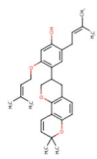
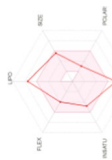
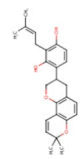

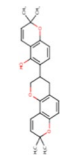
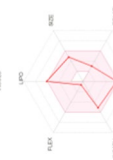
Name	MW	LogP	nHBD	nHBA	nRotB	TPSA	Lip Vio	Log Kp	EI	SA	2-D structure	Bio-rad
4'-O-Methyl pre glabridin	340.41	4.86	2	4	4	58.92	0	-4.93	0.42	3.86		
4'-O-prenyl glabridin	392.49	5.71	1	4	4	47.92	0	-4.64	0.46	4.53		
4'-O-methyl glabridin	338.40	4.21	2	5	2	68.15	0	-5.72	0.43	4.19		
3'-hydroxy-4'methoxy glabridin	354.40	3.86	2	5	2	68.15	0	-5.72	0.43	4.19		
2'-O-methylglabridin	338.40	4.21	1	4	2	97.72	0	-5.38	0.45	4.15		
2'-O,5'-C-diprenylglabridin	460.60	7.64	1	4	6	47.92	1	-3.69	0.47	5.10		
Hispaglabridin A	392.49	5.82	2	4	3	58.92	0	-4.56	0.63	4.58		
Hispaglabridin B	390.47	5.17	1	4	1	47.92	0	-5.01	0.42	4.45		

Table 3 (continued)

MW Molecular weight, *LogP* Log of octanol/water partition coefficient, *nHBA* Number of hydrogen bond acceptor (s), *nHBD* Number of hydrogen bond donor (s), *nRotB* Number of rotatable bonds, *Log Kp* Log of skin permeability, *TPSA* Total Polar surface area, *EI* Enzyme inhibition, *SA* Synthetic accessibility, *2D-Structure*- 2-dimensional structure, *Bio-RAD* Bioavailability Radar (6 vertices represents six parameters- Lipophilicity, Size, Polarity, solubility and flexibility). Range of standard values for drug like molecule: Lipophilicity- 0.7 < LogP3 < + 5.0; size— 150 g/mol < MV < 500 g/mol, polar-20A² < TPSA < 130 A²; Insolubility- 0.25 < FractionCsp3 < 1; flexibility- 0 < no of rotatable bond < 9

Comparison of Tyr (apo-protein) with Tyr in complex with Kojic acid, glabridin and its derivatives

Comparative analysis of simulated trajectories of native protein, control ligand kojic acid and 5'-formylglabridin, glabridin, 5' prenylglabridin, (R)—Glabridin and 3' hydroxy—4' methoxyglabridin were analysed in terms of root mean square deviation (RMSD), root mean square fluctuation (RMSF) and Radius of gyration (Rg) and Solvent Accessible Surface Area (SASA) plots with respect to time. The MD simulations studies were used to compare the binding of Glabridin and its derivatives with tyrosinase. The RMSD of backbone showed slight increase at initial stages, which was stabilized later during the course of simulation (Fig. 8A). Comparative RMSD analysis suggested that the binding of ligands molecules stabilises the TYR structure compared to the RMSD observed in apo-protein. The average RMSD of backbone was highest for TYR itself in comparison to TYR in complex with different ligands (Table 4). It depicts more stability of the complex as lower RMSD values indicate formation of more stable complexes (Sen Gupta et al. 2020). RMSF was plotted to compare and analyse the flexibility behaviour of the complex residues. The RMSF of C-alpha atoms of protein were higher in between residues 175–275 of TYR, which is binding region for Kojic acid and its derivative, rest of the structure remained stable (Fig. 8B). Protein structure compactness and stability can correctly be defined in terms of the radius of gyration (Rg) (Bhardwaj et al. 2020; Kalhor et al. 2020). The average Rg value for apo-protein is depicted near 2.13 nm by a small fall from the initial to the end of MD simulation. The Kojic acid-TYR complex showed the small fall till 10,000 ps (Fig. 8C) after that it maintained the structural stability till the end of simulation. The average Rg for Kojic acid-TYR complex is near 2.1 nm, although the average Rg value for TYR-grabridin complex and complex of glabridin derivatives with TYR is > 2.1 nm. The decline in total SASA score confirms less availability of residues to the solvent and further compaction upon binding of the ligands, which is quite evident in the case of TYR-Kojic acid and TYR- 5' formylglabridin complex and other complexes (Fig. 8D). The decrease in total SASA is validated by decrease in the number of intramolecular hydrogen bonds (Fig. 9), since hydrogen bonds are important for stable and precise binding (Sigala et al. 2009; Qiu et al. 2018). All complex of glabridin and its derivatives with TYR appears more reliable and stable in terms of RMSD, RMSF and Rg in comparison to Kojic acid complexed with TYR. Comparative analysis of SASA results of tyrosinase and its complex with kojic acid and other complexes suggested that glabridin and its derivatives are the stable ligand which shows its potential binding to TYR. Similar analysis was performed by Umesh et al. 2021 for identifying new anti-CoV drug chemical from Indian spices targeting SARS-CoV-2 main protease.

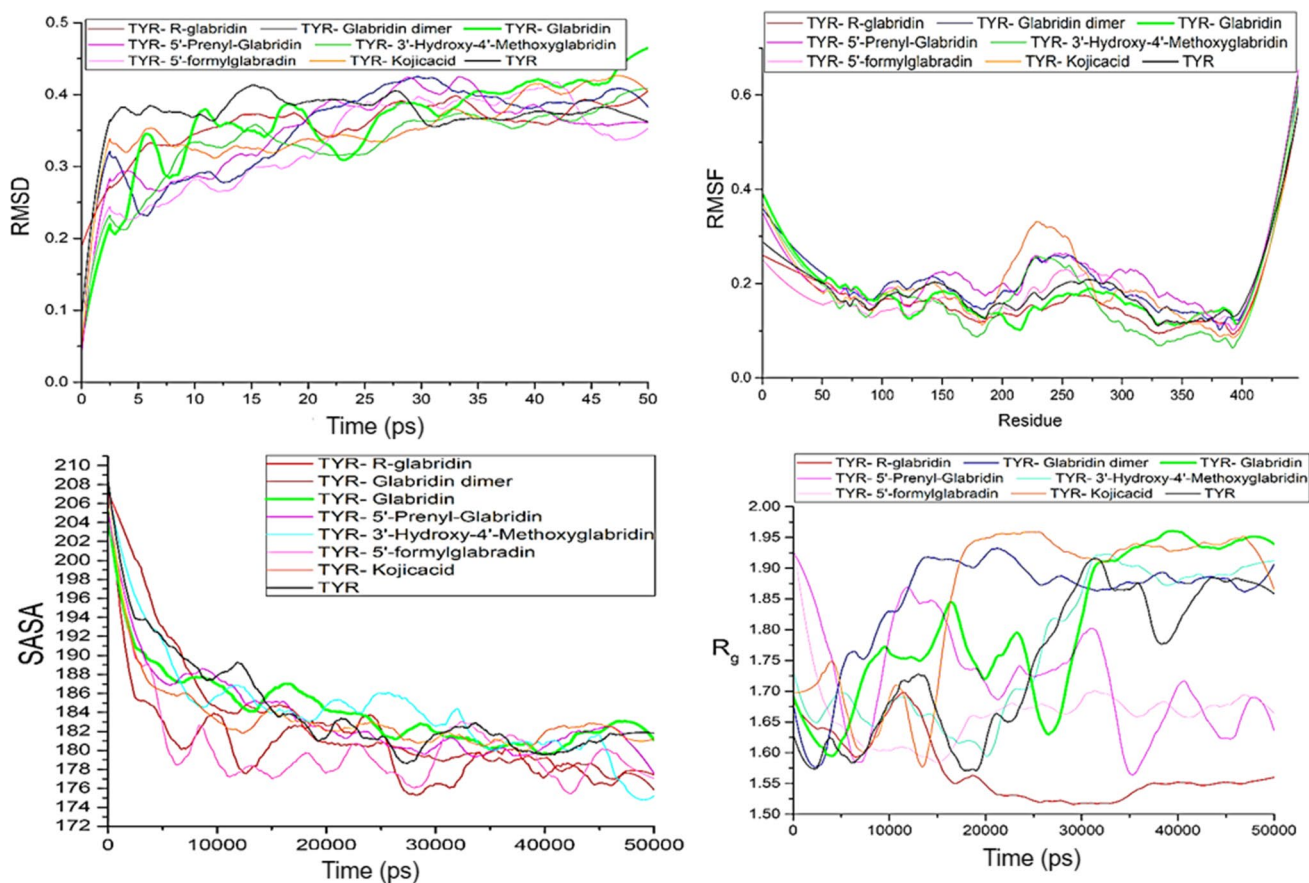


Fig. 8 Molecular dynamic simulation studies of modelled Human Tyrosinase enzyme (hTYR), control ligand kojic acid complexed with TYR and 5'-formylglabridin ligand complexed with hTYR. **A:** Graphic presentation of root mean square deviation (RMSD) of apo-proteins and complex structures. **B:** Graphic presentation of

root mean square fluctuation (RMSF) of apo-proteins and complex structures. **C:** Graphic presentation of radius of gyration (R_g) of apo-proteins and complex structures. **D:** Graphic presentation of Solvent Accessible Surface Area (SASA) of apo-proteins and complex structures

Table 4 The average RMSD of protein backbones during the molecular dynamic simulations

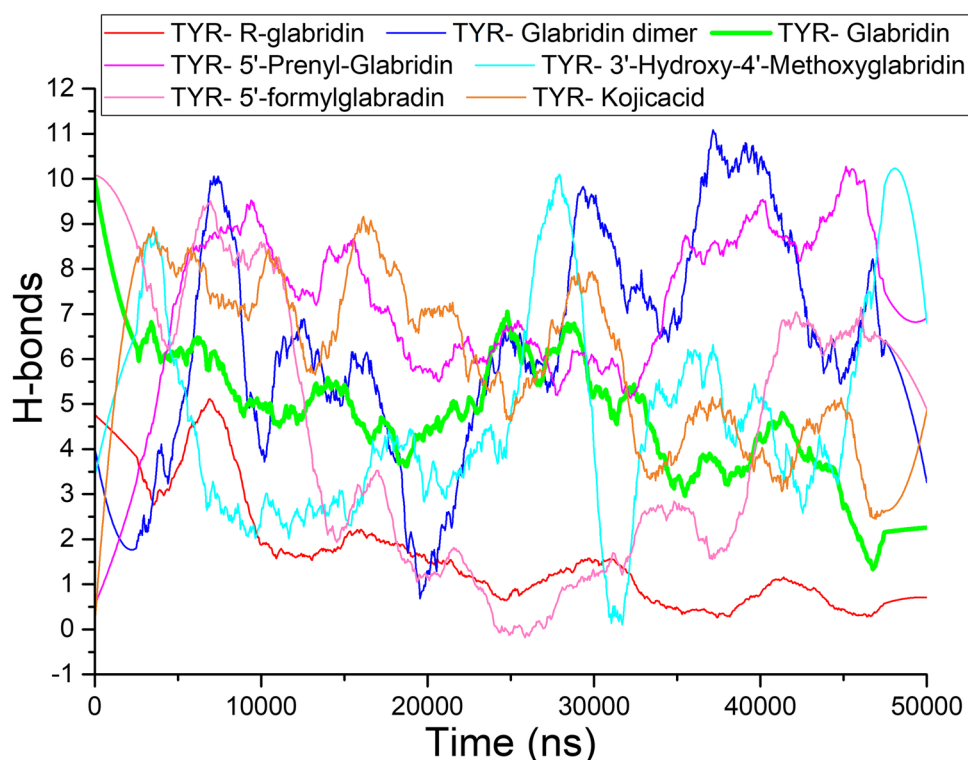
System	Average RMSD of protein Backbone
TYR (apo protein)	3.5 Å
TYR- Kojic acid	3.5 Å
TYR-5'-formylglabridin	3.2 Å
TYR-5'-prenylglabridin	3.4 Å
TYR-glabridin dimer	3.2 Å

Conclusion

The current approaches employed in identification of tyrosinase inhibitors recognises glabridin and its natural and semi-synthetic derivatives for their bioactive potential as tyrosinase inhibitor. Glabridin derivatives have not been explored for their role in tyrosinase inhibition. The primary objective

of the present study was to search for the potential and effective molecules that could inhibit tyrosinase or suppress the production of melanin so that they can be used as effective and safe skin care and cosmetic agents. Through molecular docking in virtual model of human tyrosinase (hTYR) we demonstrated the inhibitory effect of glabridin and glabridin derivatives. The glabridin derivatives molecules exhibited active binding with human tyrosinase. Manual ranking of these molecules based on the binding scores projected 5-formylglabridin as having the highest binding affinity with the docking score -9.3. HIS 338, HIS 177, HIS 342, SER 350, VAL 352, ASN 339, PHE 322, SER 330, SER 355, ILE 343, HIS 155 and ARG 171 were found to be important residues for binding of ligands in the active site of human tyrosinase model. Glabridin effectively controlled the melanin production in B16F10 melanoma cells. Even though, all the glabridin derivatives successfully docked with the modelled tyrosinase enzyme but, four molecules namely 5'-formylglabridin, glabridin dimer, (R)-Glabridin and 5'-prenylglabridin were identified as potent inhibitor of

Fig. 9 Graphic representation of Hydrogen bonding pattern of complexes of TYR enzyme with kojic acid, glabridin and its derivatives during molecular dynamic simulation



hTYR based on their higher binding affinity than glabridin. ADME properties analysis projected all studied molecules as drug candidate because they followed all criteria required for absorption, distribution, metabolism and excretion and didn't violate the rule 5. Further, molecular simulation studies also confirmed the effective binding of glabridin, 5'-formylglabridin, R- glabridin, 5'-prenylglabridin, glabridin dimer and 3'-hydroxy-4'methoxyglabridin with hTYR authenticating the binding of it for inhibition mechanism and appears better candidate than the commonly used kojic acid for hyperpigmentary conditions. However, the complete prospects of these compounds need to be explored further in wet lab studies before being used as an ingredient in anti-hyperpigmentary formulations.

Supplementary Information The online version contains supplementary material available at <https://doi.org/10.1007/s13596-022-00640-8>.

Funding Funding not available.

Data Availability The data that supports the findings of this study are available in the supplementary material of this article.

Declarations

Ethical statement This article does not contain any studies involving animals performed by any of the authors. This article does not contain any studies involving human participants performed by any of the authors.

Conflict of interest Arti Kumari has no conflict of interest. Rakesh kumar has no conflict of interest. Gira Sulabh has no conflict of interest. Pratihtha Singh has no conflict of interest. Jainendra Kumar has no conflict of interest. Vijay Kumar Singh has no conflict of interest. Krishna Kumar Ojha has no conflict of interest.

References

- Ali SA, Naaz I (2015) Current challenges in understanding the story of skin pigmentation—bridging the morpho-anatomical and functional aspects of mammalian melanocytes. *Muscle Cell Tissue* 2:262–285
- Baurin N, Arnoult E, Scior T, Do QT, Bernard P (2002) Preliminary screening of some tropical plants for anti-tyrosinase activity. *J Ethnopharmacol* 82(2–3):155–158
- Belinky PA, Aviram M, Mahmood S, Vaya J (1998) Structural aspects of the inhibitory effect of glabridin on LDL oxidation. *Free Radical Biol Med* 24(9):1419–1429
- Berendsen HJ, Postma JV, van Gunsteren WF, DiNola AR, Haak JR (1984) Molecular dynamics with coupling to an external bath. *J Chem Phys* 81(8):3684–3690
- Berendsen HJ, van der Spoel D, van Drunen R (1995) GROMACS: a message-passing parallel molecular dynamics implementation. *Comput Phys Commun* 91(1–3):43–56
- Berman H, Henrick K, Nakamura H, Markley JL (2007) The worldwide protein data bank (wwPDB): ensuring a single, uniform archive of PDB data. *Nucleic Acids Res* 35(suppl_1):D301–D303
- Bhardwaj VK, Singh R, Sharma J, Rajendran V, Purohit R, Kumar S (2020) Identification of bioactive molecules from tea plant as SARS-CoV-2 main protease inhibitors. *J Biomol Struct Dyn* 20:1

- Borges CR, Roberts JC, Wilkins DG, Rollins DE (2001) Relationship of melanin degradation products to actual melanin content: application to human hair. *Anal Biochem* 290(1):116–125
- Cavaliere EL, Li KM, Balu N, Saeed M, Devanesan P, Higginbotham S, Zhao J, Gross ML, Rogan EG (2002) Catechol ortho-quinones: the electrophilic compounds that form depurinating DNA adducts and could initiate cancer and other diseases. *Carcinogenesis* 23(6):1071–1077
- Cestari TF, Dantas LP, Boza JC (2014) Acquired hyperpigmentations. *An Bras Dermatol* 89(1):11–25
- Chen J, Yu X, Huang Y (2016) Inhibitory mechanisms of glabridin on tyrosinase. *Spectrochim Acta Part A Mol Biomol Spectrosc* 168:111–117
- Choi EM (2005) The licorice root derived isoflavan glabridin increases the function of osteoblastic MC3T3-E1 cells. *Biochem Pharmacol* 70(3):363–368
- Combet C, Blanchet C, Geourjon C, Deleage G (2000) NPS@: network protein sequence analysis. *Trends Biochem Sci* 25(3):147–150
- Cui YM, Ao MZ, Li W, Yu LJ (2008) Effect of glabridin from *Glycyrrhiza glabra* on learning and memory in mice. *Planta Med* 74(04):377–380
- da Silva AP, Silva ND, Andrade EH, Gratieri T, Setzer WN, Maia JG, da Silva JK (2017) Tyrosinase inhibitory activity, molecular docking studies and antioxidant potential of chemotypes of *Lippia origanoides* (Verbenaceae) essential oils. *PLoS ONE* 12(5):e0175598
- Daina A, Michielin O, Zoete V (2017) SwissADME: a free web tool to evaluate pharmacokinetics, drug-likeness and medicinal chemistry friendliness of small molecules. *Sci Rep* 7(1):1–3
- Damle M (2014) *Glycyrrhiza glabra* (Licorice)-a potent medicinal herb. *Int J Herb Med* 2(2):132–136
- DeLano WL (2002) Pymol: an open-source molecular graphics tool. *CCP4 News Prot Crystallogr* 40(1):82–92
- Friedman M (1996) Food browning and its prevention: an overview. *J Agric Food Chem* 44(3):631–653
- Fukai T, Sakagami H, Toguchi M, Takayama F, Iwakura I, Atsumi T, Ueha T, Nakashima H, Nomura T (2000) Cytotoxic activity of low molecular weight polyphenols against human oral tumor cell lines. *Anticancer Res* 20(4):2525–2536
- Fukai T, Marumo A, Kaitou K, Kanda T, Terada S, Nomura T (2002) Anti-*Helicobacter pylori* flavonoids from licorice extract. *Life Sci* 71(12):1449–1463
- García-Borrón, Solano F (2002) Molecular anatomy of tyrosinase and its related proteins: beyond the histidine-bound metal catalytic centre. *Pigment Cell Res* 15(3):162–173
- Greggio E, Bergantino E, Carter D, Ahmad R, Costin GE, Hearing VJ, Clarimon J, Singleton A, Eerola J, Hellström O, Tienari PJ (2005) Tyrosinase exacerbates dopamine toxicity but is not genetically associated with Parkinson's disease. *J Neurochem* 93(1):246–256
- Gupta VK, Fatima A, Faridi U, Negi AS, Shanker K, Kumar JK, Rahuja N, Luqman S, Sisodia BS, Saikia D, Darokar MP (2008) Antimicrobial potential of *Glycyrrhiza glabra* roots. *J Ethnopharmacol* 116(2):377–380
- Hasegawa T (2010) Tyrosinase-expressing neuronal cell line as in vitro model of Parkinson's disease. *Int J Mol Sci* 11(3):1082–1089
- Haudecoeur R, Carotti M, Gouron A, Maresca M, Buitrago E, Hardré R, Bergantino E, Jamet H, Belle C, Réglie M, Bubacco L (2017) 2-Hydroxypyridine-n-oxide-embedded aurones as potent human tyrosinase inhibitors. *ACS Med Chem Lett* 8(1):55–60
- Hayashi H, Hattori S, Inoue K et al (2003) Field survey of *Glycyrrhiza* plants in Central Asia (3). Chemical characterization of *G. glabra* collected in Uzbekistan. *Chem Pharm Bull* 51:1338–1340
- Hsu YL, Wu LY, Hou MF, Tsai EM, Lee JN, Liang HL, Jong YJ, Hung CH, Kuo PL (2011) Glabridin, an isoflavan from licorice root, inhibits migration, invasion and angiogenesis of MDA-MB-231 human breast adenocarcinoma cells by inhibiting focal adhesion kinase/Rho signaling pathway. *Mol Nutr Food Res* 55(2):318–327
- Ibrahim ZY, Uzairu A, Shallangwa G, Abechi S (2020) Molecular docking studies, drug-likeness and in-silico ADMET prediction of some novel β -Amino alcohol grafted 1, 4, 5-trisubstituted 1, 2, 3-triazoles derivatives as elevators of p53 protein levels. *Sci Afr* 10:e00570
- Isah T (2019) Stress and defense responses in plant secondary metabolites production. *Biol Res*. <https://doi.org/10.1186/s40659-019-0246-3>
- Johnson M, Zaretskaya I, Raytselis Y, Merezhuk Y, McGinnis S, Madden TL (2008) NCBI BLAST: a better web interface. *Nucleic Acids Res* 36(suppl_2):W5–9
- Kalhor H, Sadeghi S, Marashiyani M, Kalhor R, Aghaei Gharehbolagh S, Akbari Eidgahi MR, Rahimi H (2020) Identification of new DNA gyrase inhibitors based on bioactive compounds from streptomycetes: structure-based virtual screening and molecular dynamics simulations approaches. *J Biomol Struct Dyn* 38(3):791–806
- Kobayashi T, Vieira WD, Potterf B, Sakai C, Imokawa G, Hearing VJ (1995) Modulation of melanogenic protein expression during the switch from eu-to pheomelanogenesis. *J Cell Sci* 108(6):2301–2309
- Kumari A, Kumar J (2019a) Phyto-chemical screening of root extracts of *Glycyrrhiza glabra* by spectroscopic methods (UV-VIS spectrophotometer, FTIR and HPLC). *Int J Pharm Sci Drug Res* 11(6):376–381
- Kumari A, Kumar M, Sahoo GC, Kumar J (2019b) In silico prediction of Glabridin potency against Human Tyrosinase in hyperpigmentation condition. *Int J Res Anal Rev* 6(2):332–341
- Kumari A, Kumar P, Kumar M, Kumar J (2020) Antibacterial activity of *Glycyrrhiza glabra* root extracts against *Staphylococcus* sp And *Escherichia coli*. *World J Pharm Res* 9(15):1069–1080. <https://doi.org/10.20959/wjpr202015-19285>
- Kumari A, Kumar P, Kumar M, Kumar J (2021) In silico analysis of Forskolol as a potential inhibitor of SARS-CoV-2. *J Pure Appl Microbiol* 15(2):709–715. <https://doi.org/10.22207/JPAM.15.2.22>
- Lai X, Wichers HJ, Soler-Lopez M, Dijkstra BW (2017) Structure of human tyrosinase related protein 1 reveals a binuclear zinc active site important for melanogenesis. *Angew Chem Int Ed* 56(33):9812–9815
- Lee JY, Lee J, Min D, Kim J, Kim HJ, No KT (2020) Tyrosinase-targeting gallacetophenone inhibits melanogenesis in melanocytes and human skin-equivalents. *Int J Mol Sci* 21(9):3144
- Lim TK (2016) *Glycyrrhiza glabra*. Edible medicinal and non-medicinal plants. Springer, Dordrecht, pp 354–457
- Lima CR, Silva JR, De Cardoso ÉTC, Silva EO, Lameira J, Do Nascimento JL, Do Brasil DSB, Alves CN (2014) Combined kinetic studies and computational analysis on kojic acid analogs as tyrosinase inhibitors. *Molecules* 19(7):9591–9605
- Liu SH, Pan IH, Chu IM (2007) Inhibitory effect of p-hydroxybenzyl alcohol on tyrosinase activity and melanogenesis. *Biol Pharm Bull* 30(6):1135–1139
- Masum MN, Yamauchi K, Mitsunaga T (2019) Tyrosinase inhibitors from natural and synthetic sources as skin-lightening agents. *Rev Agric Sci* 7:41–58
- Matoba Y, Kumagai T, Yamamoto A, Yoshitsu H, Sugiyama M (2006) Crystallographic evidence that the dinuclear copper center of tyrosinase is flexible during catalysis. *J Biol Chem* 281(13):8981–8990
- Mayer AM (1986) Polyphenol oxidases in plants-recent progress. *Phytochemistry* 26(1):11–20

- Millan S, Satish L, Bera K, Susrisweta B, Singh DV, Sahoo H (2017) A spectroscopic and molecular simulation approach toward the binding affinity between lysozyme and phenazinium dyes: an effect on protein conformation. *J Phys Chem B* 121(7):1475–1484
- Mushtaq S, Abbasi BH, Uzair B, Abbasi R (2018) Natural products as reservoirs of novel therapeutic agents. *EXCLI J* 17:420
- Nithitanakool S, Pithayanukul P, Bavovada R, Saparpakorn P (2009) Molecular docking studies and anti-tyrosinase activity of Thai mango seed kernel extract. *Molecules* 14(1):257–265
- Nokinsee D, Shank L, Lee VS (2015) Nimmanpipug P (2015) Estimation of inhibitory effect against tyrosinase activity through homology modeling and molecular docking. *Enzyme Res*. <https://doi.org/10.1155/2015/262364>
- Oikawa T, Yanagimachi R, Nicolson GL (1973) Wheat germ agglutinin blocks mammalian fertilization. *Nature* 241(5387):256–259
- Pettersen EF, Goddard TD, Huang CC, Couch GS, Greenblatt DM, Meng EC, Ferrin TE (2004) UCSF Chimera—a visualization system for exploratory research and analysis. *J Comput Chem* 25(13):1605–1612
- Pillaiyar T, Manickam M, Namasivayam V (2017) Skin whitening agents: medicinal chemistry perspective of tyrosinase inhibitors. *J Enzyme Inhib Med Chem* 32(1):403–425
- Pillaiyar T, Namasivayam V, Manickam M, Jung SH (2018) Inhibitors of melanogenesis: an updated review. *J Med Chem* 61(17):7395–7418
- Pol-Fachin L, Fernandes CL, Verli H (2009) GROMOS96 43a1 performance on the characterization of glycoprotein conformational ensembles through molecular dynamics simulations. *Carbohydr Res* 344(4):491–500
- Qiu M, Zhai L, Cui J, Fu B, Li M, Hou Q (2018) Diffusion behavior of hydrogen isotopes in tungsten revisited by molecular dynamics simulations. *Chin Phys B* 27(7):073103
- Radhakrishnan N, Ashok S, Kavitha V, Rameshkumar G, Gnanamani A (2013) Molecular docking studies of embelin (simple natural benzoquinone) and its derivatives as a potent tyrosinase inhibitor. *J Chem Pharm Res* 5(10):320–326
- Raper HS (1928) The aerobic oxidases. *Physiol Rev* 8(2):245–282
- Saitoh T, Kinoshita T, Shibata S (1976) New isoflavan and flavanone from licorice root. *Chem Pharm Bull* 24(4):752–755
- Schüttelkopf AW, Van Aalten DM (2004) PRODRG: a tool for high-throughput crystallography of protein–ligand complexes. *Acta Crystallogr D Biol Crystallogr* 60(8):1355–1363
- Sen Gupta PS, Biswal S, Panda SK, Ray AK, Rana MK (2020) Binding mechanism and structural insights into the identified protein target of COVID-19 and importin- α with in-vitro effective drug ivermectin. *J Biomol Struct Dyn* 27:1
- Shi YL, Benzie IF, Buswell JA (2002) Role of tyrosinase in the genoprotective effect of the edible mushroom. *Agaricus Bisporus* *Life Sci* 70(14):1595–1608
- Sigala PA, Tsuchida MA, Herschlag D (2009) Hydrogen bond dynamics in the active site of photoactive yellow protein. *Proc Natl Acad Sci* 106(23):9232–9237
- Simmler C, Pauli GF, Chen SN (2013) Phytochemistry and biological properties of glabridin. *Fitoterapia* 1(90):160–184
- Tessari I, Bisaglia M, Valle F, Samori B, Bergantino E, Mammi S, Bubacco L (2008) The reaction of α -synuclein with tyrosinase: possible implications for Parkinson disease. *J Biol Chem* 283(24):16808–16817
- Tian W, Chen C, Lei X, Zhao J, Liang J (2018) CASTp 3.0: computed atlas of surface topography of proteins. *Nucleic Acids Res* 46(W1):W363–W367. <https://doi.org/10.1093/nar/gky473>
- Trott O, Olson AJ (2010) AutoDock Vina: improving the speed and accuracy of docking with a new scoring function, efficient optimization, and multithreading. *J Comput Chem* 31(2):455–461
- Umesh, Kundu D, Selvaraj C, Singh SK, Dubey VK (2021) Identification of new anti-nCoV drug chemical compounds from Indian spices exploiting SARS-CoV-2 main protease as target. *J Biomol Struct Dyn* 39(9):3428–3434
- Vontzalidou A, Zoidis G, Chaita E, Makropoulou M, Aligiannis N, Lambrinidis G, Mikros E, Skaltsounis AL (2012) Design, synthesis and molecular simulation studies of dihydrostilbene derivatives as potent tyrosinase inhibitors. *Bioorg Med Chem Lett* 22(17):5523–5526
- Wallace AC, Laskowski RA, Thornton JM (1995) LIGPLOT: a program to generate schematic diagrams of protein–ligand interactions. *Protein Eng Des Sel* 8(2):127–134
- Webb B, Lasker K, Velázquez-Muriel J, Schneidman-Duhovny D, Pellarin R, Bonomi M, Greenberg C, Raveh B, Tjioe E, Russel D, Sali A (2014) Modeling of proteins and their assemblies with the integrative modeling platform. In *Structural Genomics*. Humana Press, Totowa, pp 277–295
- Yi W, Cao R, Peng W, Wen H, Yan Q, Zhou B, Ma L, Song H (2010) Synthesis and biological evaluation of novel 4-hydroxybenzaldehyde derivatives as tyrosinase inhibitors. *Eur J Med Chem* 45(2):639–646
- Yokota T, Nishio H, Kubota Y, Mizoguchi M (1998) The inhibitory effect of glabridin from licorice extracts on melanogenesis and inflammation. *Pigment Cell Res* 11(6):355–361
- Yu XQ, Xue CC, Zhou ZW, Li CG, Du YM, Liang J, Zhou SF (2008) In vitro and in vivo neuroprotective effect and mechanisms of glabridin, a major active isoflavan from *Glycyrrhiza glabra* (licorice). *Life Sci* 82(1–2):68–78

Publisher's Note Springer Nature remains neutral with regard to jurisdictional claims in published maps and institutional affiliations.